

## APPLICATION OF HTS WIRE TO MAGNETS \*

K. Hatanaka<sup>#</sup>, M. Fukuda, J. Nakagawa, T. Saito, T. Yorita, RCNP, Ibaraki, 567-0047 Osaka, Japan  
 Y. Sakemi, CYRIC, Sendai, 980-8578 Miyagi, Japan  
 T. Kawaguchi, KT Science Ltd., Akashi, 673-0044 Hyogo, Japan  
 K. Noda, NIRS, Inage, 263-8555 Chiba, Japan

### Abstract

We have been developing magnets utilizing high-temperature superconducting (HTS) wire. A scanning magnet was designed, fabricated, and tested for its suitability as beam scanner. After successful cooling tests, the magnet performance was studied using DC and AC currents. In AC mode, the magnet was operated at frequencies of 30-59Hz and a temperature of 77K as well as 10-20Hz and 20K. The power loss dissipated in the coils was measured and compared with the model calculations. The observed loss per cycle was independent of the frequency and the scaling law of the excitation current was consistent with theoretical predictions for hysteretic losses in HTS wires. As the next step, a 3T dipole magnet is under construction now.

### INTRODUCTION

More than two decades have passed since the discovery of high-temperature superconductor (HTS) materials in 1986 [1]. Significant effort went into the development of new and improved conductor materials [2] and it became possible to manufacture relatively long HTS wires of the first generation [3]. Although many prototype devices using HTS wires have been developed, these applications are presently rather limited in accelerator and beam line facilities [4].

Our previous study demonstrated a possibility to excite HTS magnets with alternating currents (AC) [5]. Since HTS systems have higher operating temperatures than low-temperature superconductor (LTS) systems, the cryogenic components for cooling are simpler and the cooling power of refrigerators is much larger than at 4K. Because the temperature range for superconductivity is wider than for LTS systems, a larger range of operating temperatures is available. A high-frequency AC mode operation should be possible in spite of heating loads due to AC losses in the coils.

A two-dimensional scanning magnet was designed and built to model a compact system for such applications as ion implantation or particle cancer treatment. Two sets of single-stage GM (Gifford-McMahon) refrigerators were used to cool the coils and the thermal shields. After performance tests of the design parameters with direct currents (DC), the magnet was operated with AC current to investigate the dissipated losses in the coils. Observed AC losses are compared with theoretical predictions and model calculations.

A 3T dipole magnet is under construction to continue

developments. It is a super-ferric magnet and the coil has a negative curvature..

### SCANNING MAGNET

#### Design and Fabrication

A two-dimensional scanning magnet was designed to model a compact beam scanning system. The size of the irradiation field is 200mm by 200mm for 230MeV protons at the distance of 1.25m from the magnet center. The schematic layout of the coils is shown in Fig. 1. Both the  $B_x$  and  $B_y$  coils are centered at the same position along the beam axis. The required magnetic field length is 0.185 Tm. We selected the high temperature superconductor Bi-2223 [6] that is commercially available in lengths longer than 1000m. The HTS wire consists of a flexible composite of Bi-2223 filaments in a silver alloy matrix with a thin stainless steel lamination that provides mechanical stability and transient thermal conductivity. The wire, High Strength Wire, was supplied by American Superconductor Corporation [7] and is in thin tape-form approximately 4.2mm wide and 0.26mm thick.

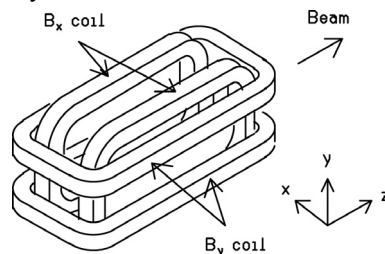


Figure 1: A schematic layout of the scanning magnet coils is shown. They generate the horizontal ( $B_x$ ) and vertical ( $B_y$ ) magnetic fields.

Table 1: Design parameters of the HTS scanning magnet.

Coils	Iner size	$B_x$ : 150mm x 300mm.
		$B_y$ : 150mm x 380mm
	Separation	70mm
	Maximum Field	0.6T
	# of turns	420 x 2 for $B_x$ and $B_y$
	Winding	3 Double pancakes/coil
	Inductance/coil	$B_x$ : 75mH, $B_y$ : 92mH
	Temperature	20K
	Rated current	200A
Cryostat	Cooling power	45W at 20K, 53W at 80K

\* hatanaka@rcnp.osaka-u.ac.jp

The scanning magnet consists of two sets of two racetrack-type coils. Each coil is built by stacking three double pancakes. The design parameters are summarized in Table 1. Figure 2 shows a photograph of an as

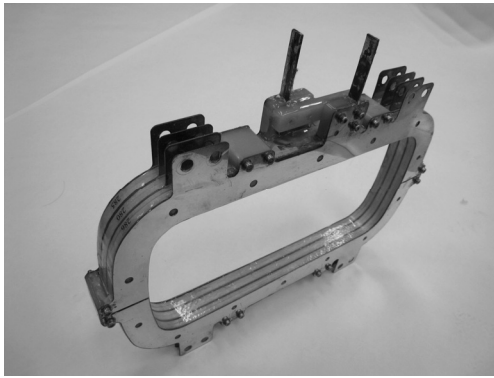


Figure 2: Photograph of single assembled Bx coil.

The critical current ( $I_c$ ) of the HTS conductor depends on the operating temperature and the magnetic field at its surface. The magnetic field perpendicular to the conductor has larger effects on  $I_c$  than the horizontal component. Before winding, the  $I_c$  of the wire over the full length was measured at 77K in a 10m pitch and found to be between 125 and 140A corresponding to an electric field amplitude of  $1\mu\text{V}/\text{cm}$ . The  $I_c$  values of the coils were estimated from the  $I_c(B_{\perp})$  characteristics of the tape conductor and a magnetic field analysis using the finite element code TOSCA. The load line of the coil was found to cross the  $I_c(B_{\perp})$  curve at 0.195T and a current of 39A corresponding to an  $I_c$  at 77K. In the present design, the maximum field was 0.6T in the center along the axis of the magnet and the required magneto-motive force is  $8.4 \times 10^4 \text{AT}$  for each coil. The maximum field perpendicular to the tape surface is estimated to be 1T. From the specification of the temperature dependence of the  $I(B_{\perp})$  characteristics, the  $I_c$  value was estimated to be 260A at 20K. The rated current of the coil was designed to be 200A to generate the field length of 0.185Tm.

### DC Performance Tests

The  $I_c$  value of each pancake was measured in a liquid nitrogen bath. They were 56-62A for all pancakes. After stacking three pancakes to form a coil, the self-field  $I_c$  of the  $B_x$  and  $B_y$  coils was measured separately. The  $I_c$  values were 40-43A and consistent with the design value of 39A described in the previous section. This demonstrated that the HTS wire was not damaged by the winding procedure and that we can expect operating currents larger than 200A at 20K.

After the installation of the magnet, the cryostat was evacuated by a turbo-molecular pump with a pumping rate of 300l/sec. Coil resistances and temperatures on the coil surfaces and shields were measured during the cooling procedure. HTS coils became superconducting at 105K after 10 hours of cooling. The final temperature below 20 K was achieved after one day of cooling. The temperature of the coils was measured by silicon diode

sensors DT-670 of Lake Shore Cryotronics Inc. at several locations. The temperature of the thermal shields was measured by thermocouples. The equilibrium temperature was about 100K at the farthest point from the cold head of the refrigerator.

The  $I_c$  values measured at 20K were 257A and 282A for the  $B_x$  and  $B_y$  coils, respectively. They were consistent with the design values. The magnetic field distribution along the central axis ( $z$ ) was measured at 100A using a Hall probe. The measured magnetic fields agreed with calculations by the code TOSCA very well.

### AC Operation

Owing to the good thermal performance we can expect a large thermal operating range for the present coils. Such a large range suggests the possibility to excite the magnet in the AC mode while maintaining superconductivity as long as the AC loss in the HTS tape is acceptable. Several AC loss components are observed in both LTS and HTS magnets [8, 9]. They are (1) hysteretic magnetization losses in the superconductor material, (2) dynamic resistance losses generated by a flux motion in the conductor, (3) coupling losses through the matrix, and (4) eddy current losses in the matrix and metallic structures including cooling plates. For HTS magnets, there are Ohmic losses at exciting currents above the critical current as well. Each AC loss shows a different dependence on the frequencies ( $f$ ), the amplitude of the external magnetic field ( $B$ ) and the transport current ( $I_t$ ). The power dissipation per cycle for each loss (1) - (4) listed above scales as

$$2 \ln[\cosh x] - x \tanh x \quad (1)$$

$$BI^2 \quad (2)$$

$$fB^2 \quad (3)$$

$$fB^2 \quad (4)$$

where  $x = B/B_{c0}$  and  $B_{c0} = \mu_0 J_c d / \pi$ .  $J_c$  is the critical current density and  $d$  thickness of the conductor tape. For such a geometry as discussed in the present study, the external magnetic fields are also generated by the transport current. In this case, the magnetic field amplitude can be expected roughly proportional to the transport current. AC losses due to the first two phenomena (1) and (2) are independent of the frequency. On the other hand, losses (3) and (4) depend linearly on the frequency.

In AC loss measurements, two  $B_x$  coils were connected in series in the cryostat and cooled down below 20K [10]. The power dissipated in the coils was measured at three frequencies, 10.5Hz, 15Hz and 21Hz. Measurements were performed using an electrical method where the voltage across coils was measured in-phase with the transport current using an oscilloscope. The system consisted of an inverter, an induction motor and a generator that was employed to convert the line frequency of 60Hz to the resonance frequencies. The inductance of a single  $B_x$  coil was measured to be 70 mH at 77K. The total inductance of two coils in series was estimated to be 170mH. Coils and condensers formed a series resonance circuit. The

capacitances of condensers in series were  $1200\mu\text{F}$ ,  $600\mu\text{F}$  and  $300\mu\text{F}$ . The resonance frequencies were roughly estimated to 10, 15 and 20Hz, respectively.

Figure 3 shows the measured AC power losses of the two  $B_x$  coils in series. The losses are roughly proportional to the 2.4th power of the transport current instead of the third power observed at 77K. The dashed curve in Fig. 5 presents the result of the finite element model analysis by T. King [10]. A close inspection of the result showed that the hysteretic and normal resistance losses were all reduced compared to calculations at 77K, but the eddy current losses in the silver alloy matrix and the brass cooling plates resulted in an overall increase of the losses. It was found that the predicted power was dominated by the losses due to eddy currents in the metallic materials. Consequently, the modelled losses were roughly proportional to the quadratic power of the transport current and the losses per cycle were linearly dependent on the frequency. In contrast, the observed dissipated power per cycle is again almost independent of the frequency of the transport current as seen in Fig. 3. The solid curve in the figure shows the theoretical  $Q_{hys}$  which is normalized to the measured value at 45A and 15Hz. At 20K,  $J_c$  of the present HTS wire is about  $5 \times 10^8 \text{A/m}^2$ . The theory is found to reproduce the scaling law well as a function of the transport current, if we take account the temperature dependence of the critical current density of the conductors.

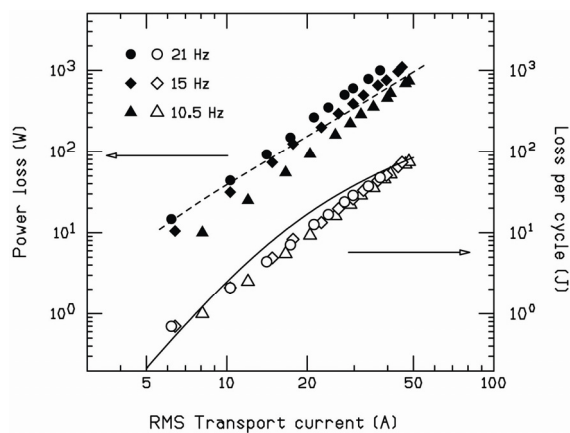


Figure 3: Measured AC losses at 20K of the  $B_x$  coils in series. Full symbols show the total power losses on the left side scale. Open symbols present losses per cycle on the right side scale. The dashed curve shows the model calculation by King [11]. The solid curve is a theoretical prediction normalized to the measured data.

### 3T DIPOLE MAGNET

In order to investigate feasibilities of synchrotron magnets using HTS wire, we are fabricating a super-ferric dipole magnet to be operated by lumping currents. The specifications are summarized in Table 2.

Table 2: Design parameters of the 3T HTS dipole magnet.

Magnet	Bending radius	400mm
	Bending angle	50deg.
	Pole gap	30mm
Coils	# of turns	600 x 2
	Winding	3 Double pancakes/coil
	Temperature	20K
	Rated current	300A

Upper and lower coils were already fabricated. Each consists of 3 double pancakes of 200 turns. Figure 4 shows double pancakes for the upper coil. Critical currents were measured of wire measured at 77K. Self-field  $I_c$  of wire was higher than 160A.  $I_c$  values of double pancakes were 60-70A. After stacking, they were 47A and 51A for the upper and lower coil, respectively. There were no damages in wire during winding process.



Figure 4: Photograph of double pancakes.

### REFERENCES

- [1] J.G. Bednorz and K.A. Müller, Physical B 64 (1986) 189.
- [2] K. Sato, K. Hayashi, K. Ohkura, K. Ohmatsu, Proc. of MT-15, Beijing (1997) 24-29.
- [3] L.J. Masur, J. Kellers, F. Li, S. Fleshler, E.R. Podtburg, Proc. of MT-17, Geneva (2001) 1-5.
- [4] D.M. Pooke, J.L. Tallon, R.G. Buckley, S.S. Kalsi, G.Snitchler, H. Picard, R.E. Schwall, R. Neale, B. MacKinnon, Proc. o CIMTEC'98, Italy (1998).
- [5] K. Hatanaka, S. Ninomiya, Y. Sakemi, T. Wakasa, T. Kawaguchi, N. Takahashi, Nucl. Instr. Meth. in Phys. Res. A 571 (2007) 583-587.
- [6] A.P. Malozemoff et al., Proc. 1998 Applied Superconductivity Conference, Palm Desert, CA, 14-19, 1998.
- [7] <http://www.amsc.com/>
- [8] C. M. Friend, "Ac losses of HTS tapes and wires", Studies of High Temperature Superconductors, A. V. Narlikar, Ed. New York: Nova Science Publishers, 2000, vol. 32, pp. 1-61.
- [9] E.H. Brandt and M. Indenbom, Phys. Rev. B 48 (1993) 12893-12906.
- [10] K. Hatanaka, J. Nakagawa, M. Fukuda, T. Yorita T..Saito, Y. Sakemi, T. Kawaguchi, K. Noda, Nucl. Instr. Meth. in Phys. Res. A 616 (2010) 16-20.
- [11] T. King, private communication.